Spin-Coated CdS Thin Films for n-Channel Thin Film Transistors

Jong-Baek Seon, Sangyoon Lee, and Jong Min Kim*

Display Device & Processing Laboratory, Samsung Advanced Institute of Technology, Mt. 14-1, Nongseo-dong, Giheung-gu, Yongin-si, Gyeongggi-do 449-712, Korea

Hyun-Dam Jeong*

Department of Chemistry, Chonnam National University, 300 Yongbong-dong, Buk-gu, Gwangju-si 500-575, Korea

Received June 10, 2008. Revised Manuscript Received December 16, 2008

Low-cost and high-performance materials fabricated at low temperatures via solution processes are of great interest in the field of printable and flexible electronics. We have investigated a new solution-based approach to the synthesis of semiconducting chalcogenide films for use in thin-film transistor (TFT) devices in an attempt to develop a simple and robust solution process for the synthesis of inorganic semiconductors. Our material design strategy is to use a sol−gel reaction for the deposition of a spin-coated CdS film that can then be converted to a xerogel material. By carrying out the spin-coating of a $L_2Cd(S(CO)CH_3)_2$ (L = 3,5-lutidine) precursor, which condenses at low temperatures to form a CdS network, and then hard-baking at 300 °C under atmospheric pressure, microscopically flat films were successfully obtained. To determine the field effect mobilities of the spin-coated CdS films, we constructed TFTs with an inverted structure consisting of Mo gate electrodes and ZrO_2 gate dielectrics. These devices exhibited n-channel TFT characteristics with an excellent field-effect mobility (a saturation mobility of ~48 cm^2V^{-1} s^{-1}) and a low voltage operation (<5 V), indicating that these semiconducting thin film materials can be used in low-cost and high-performance printable electronics.

Introduction

Solution-based processes such as spin-coating, dip-coating, and ink-jet printing enable low-cost and large-area fabrication on plastic substrates. The primary use of these methods lies in the processing of organic materials such as poly(3-hexylthiophene), which have been found to exhibit field effect mobilities of ~0.1 cm^2 V^{-1} s^{-1}.[1] Mobilities as high as 0.89 cm^2 V^{-1} s^{-1} have been achieved in p-type thin film transistor (TFT) channels consisting of solution-based pentacene.[2] In addition, in order to realize the low-cost portable devices, complementary metal oxide semiconductor (CMOS) circuits operating at sufficient speeds with low power dissipation need to be developed, which requires solution-processed n-channel TFTs.[3] Soluble polymers and molecular organic compounds have some disadvantages, including poor thermal and mechanical stabilities, and as such, are less common for n-type semiconductors. Their mobility is fundamentally limited by the weak van der Waals interactions between the organic molecules.[4] To produce low-cost and flexible I/O screens for computers constructed entirely on plastic and radio frequency identification (RFID) tags, we need to achieve thin film mobilities greater than 10 cm^2 V^{-1} s^{-1}. Furthermore, it has been reported that mobilities greater than 200 cm^2 V^{-1} s^{-1}, at a process temperature of less than 200 °C on plastic substrates, could be used to integrate peripheral circuits such as driver ICs and made to drive the pixels of active matrix organic light-emitting diodes (AMOLEDs).[5]

Solution-processed inorganic semiconductors have recently been investigated in an attempt to produce TFTs with high mobilities.[4] Inorganic semiconductors can have intrinsic mobilities as high as ~1000 cm^2 V^{-1} s^{-1}; however, they are known for their intrinsic insolubility in most solvents commonly used in solution processing. To overcome this obstacle, researchers have pursued several approaches in recent years. Mitzi et al. developed a method in which hydrazinium-based selenide salts are dissolved in organic solvents such as amines or DMSO, whereby the $M_2Se_6^{4-}$ (M = Ge, Sn) anions and hydrazinium cations are stabilized by strong hydrogen bonding interactions.[6] The hydrazinium cations dissociate from the structure upon heating to approximately 200 °C in an inert atmosphere with a crystalline metal selenide forms above 300 °C. Mitzi et al. also reported a TFT mobility of 12.0 cm^2 V^{-1} s^{-1} for chalcogenide thin films synthesized by a spin-coating method employing

* Corresponding author. E-mail: hdjeong@chonnam.ac.kr (H.-D.J.); jongkim@samsung.com (J.M.K.). Fax: 82-62-530-3389 (H.-D.J.); 82-31-280-9349 (J.-M.K.). Tel: 82-62-530-3387(H.-D.J.); 82-31-280-9311(J.-M.K.).

(1) Sirringhaus, H.; Tessler, N.; Friend, R. H. *Science* **1998**, *280*, 1741.
(2) Afzali, A.; Dimitrakopoulus, C. D.; Breen, T. L. *J. Am. Chem. Soc.* **2002**, *124*, 8812.
(3) Yoo, B.; Jones, B. A.; Basu, D.; Fine, D.; Jung, T.; Mohapatra, S.; Facchetti, A.; Dimmler, K.; Wasielewski, M. R.; Marks, T. J.; Dodabalapur, A. *Adv. Mater.* **2007**, *19*, 4028.
(4) Mitzi, D. B. *J. Mater. Chem.* **2004**, *14*, 2355.
(5) Kim, D. Y. High performance Poly-Si thin film transistor on plastic substrate. *Proceedings of the 12th International Workshop on Active-Matrix Liquid-Crystal Displays*, Kanazawa, Japan, July 6−8, 2005; Japan Society of Applied Physics: Tokyo, 2005; p 299.
(6) Mitzi, D. B. *Inorganic chemistry* **2004**, *44*, 3755.

10.1021/cm801557q CCC: $40.75
Published on Web 01/20/2009

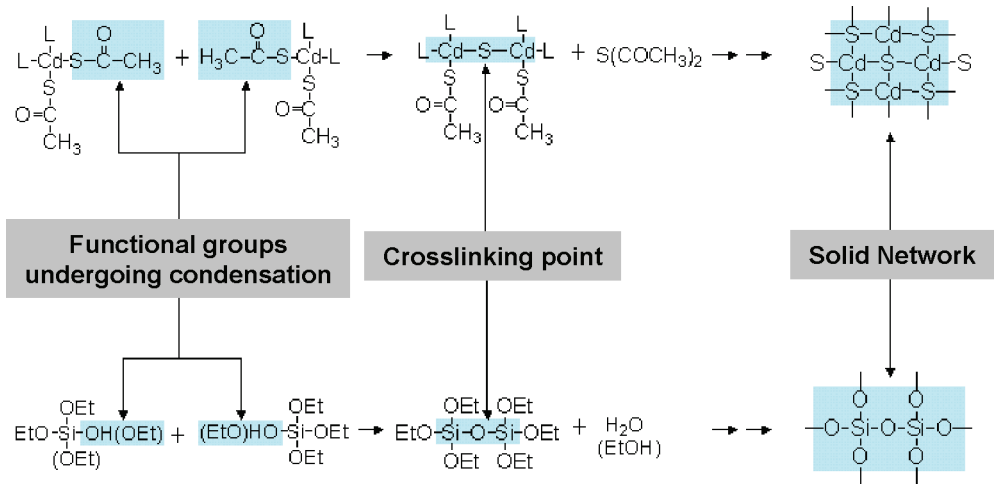

Figure 1. Reaction scheme showing the similarity of the condensation polymerizations of $L_2Cd(S(CO)CH_3)_2$ (L = 3,5-lutidine) and tetraethylorthosilicate (TEOS).

hydrazinium-based salts.[7] However, the annealing process in their method must be carried out in a nitrogen-filled dry box with oxygen and water levels below 1.0 ppm, which reduces the usefulness of this approach in the fabrication of spin-coated inorganic semiconductors for low-cost, large-area displays. In another approach, Ridely et al. and Talapin et al. investigated TFTs containing inorganic semiconductors produced from chalcogenide nanocrystal solutions.[8,9] In the experiments of Ridely et al., CdSe nanocrystals were loosely capped with pyridine molecules and readily desorbed to leave organic-free nanocrystals. TFTs containing these nanocrystalline films processed at 350 °C were found to exhibit a field effect mobility of 1.0 $cm^2\ V^{-1}\ s^{-1}$ with hysteresis behavior due to the interface states at the semiconductor/insulator interface. The TFT devices not encapsulated did not exhibit any field effect, implying degradation upon exposure to air. In the study of Talapin et al., a higher electron mobility near 2.5 $cm^2\ V^{-1}\ s^{-1}$ was realized through the thermal activation of PbSe nanocrystal films and the saturation of the dangling bonds at the nanocrystal surface with lone pairs of electrons via hydrazine treatment.

In an attempt to develop a simple and robust solution process for the synthesis of inorganic semiconductors, an alternative solution-based approach toward the synthesis of semiconducting chalcogenide films for TFT devices was investigated. Our new material design strategy is to use a sol−gel reaction to carry out the deposition of spin-coated CdS films. Most syntheses of spin-coated silicon oxide materials are based on sol−gel processes with tetraethylorthosilicate (TEOS), comprising a hydrolysis reaction and a condensation polymerization,[10] as shown below.

Hydrolysis reaction

$$Si(OEt)_4 + xH_2O \rightarrow Si(OH)_x(OEt)_{4-x} + xROH \quad (1)$$

Condensation reaction

$$-Si-(OEt) + -Si(OH) \rightarrow -Si-O-Si- + EtOH \quad (2a)$$

$$-Si-(OH) + -Si(OH) \rightarrow -Si-O-Si- + H_2O \quad (2b)$$

This condensation polymerization produces a wet gel consisting of a three-dimensional solid network with liquid-filled pores. When the pore liquid is replaced with air, without intrinsically altering the network structure by use of a supercritical drying method, a SiO_2 aerogel with a low bulk density (0.004−0.500 g/cm^3) is obtained.[11] Conversely, a SiO_2 xerogel with a higher bulk density is formed upon conventional drying, in which the wet gel shrinks significantly as a result of the capillary forces acting on the pore walls that arise as the liquid retreats from the porous network.[11] This sol−gel process for the synthesis of SiO_2 materials occurs when the ethoxy groups ($-OCH_2CH_3$) of the TEOS molecules are converted to hydroxy groups (−OH) in the hydrolysis reaction step. The hydroxy groups condense with other adjacent hydroxy or ethoxy groups to form a structure consisting of Si−O−Si bridges. In this paper, it is demonstrated that, for tetraethylorthosilicate (TEOS), the condensation polymerization of metal chalcogenide molecules with condensable ligands can give rise to a metal chalcogenide solid network structure with semiconducting properties. The metal chalcogenide network can then be converted into a metal chalcogenide aerogel or xerogel depending on the drying method. One important aspect of the proposed study was to find a suitable chalcogen (S, Se) containing functional groups that enable condensation polymerizations. Within the TEOS molecule, this role is played by the ethoxy groups. It has been shown that the thioacetic ligands ($-S(CO)CH_3$) in $L_2Cd(S(CO)CH_3)_2$ (L = 3,5-lutidine) undergo condensation polymerization and result in the formation of thioacetic anhydride ($S(COCH_3)_2$) in a relatively low temperature range, 125−150 °C.[12] This process is easily understood by comparison with the condensation polymerization of TEOS, as shown in Figure 1. The fact that the reaction proceeds at low temperatures is very important for the flexible substrates used in large-area display applications. On the other hand, the role and fate of the lutidine ligands in the precursor have to also be described in order to clarify the above condensation mechanism. In

(7) Mitzi, D. B.; Kosbar, L. L.; Murray, C. E.; Copel, M.; Afzali, A. *Nature* **2004**, *428*, 299.
(8) Ridley, B. A.; Nivi, B.; Jacobson, J. M. *Science* **1999**, *286*, 746.
(9) Talapin, D. V.; Murray, C. B. *Science* **2005**, *310*, 86.
(10) Mitzi, D. B. *Chem. Mater.* **2001**, *13*, 3283.
(11) Hüsing, N.; Schubert, U. *Angrew. Chem., Int. Ed.* **1998**, *37*, 22.
(12) Nyman, M. D.; Hampden-Smith, M. J.; Duesler, E. N. *Inorg. Chem.* **1997**, *36*, 2218.

the original study of the $L_2Cd(S(CO)CH_3)_2$ (L = 3,5-lutidine) compound,[12] the authors held that pre-equilibrium dissociation of lutidine was followed by intermolecular, rate-determining thioacetic anhydride elimination. They also proposed that the decomposition reaction of the cadmium compounds took place from 25 to 110 °C, in pyridine solvent, to form CdS nanoclusters, where the lutidine ligands act as a surface-capping reagent that retards growth of the nanoclusters. Subsequently, it is the contention of the authors that the stabilized CdS nanoclusters capped with thioacetic groups and lutidine ligands exist partially with the pure molecular precursor ($L_2Cd(S(CO)CH_3)_2$ (L = 3,5-lutidine)) in the spin-coating solution made at room temperature. Thus, in terms of the sol−gel reaction concept, the stabilized CdS nanocluster and pure molecular precursor act as sol colloidal particles in a sol solution, which can be used for the spin-coated, semiconducting film. The thioacetic groups can polymerize the CdS nanoclusters in spin-coated films by surrounding the pure molecular precursor or other CdS nanoclusters at baking temperatures of 100−300 °C, verifying the synthesis of a CdS xerogel film using the conventional drying method. Herein, the authors propose the possibility of the sol−gel process using a $L_2Cd(S(CO)CH_3)_2$ (L = 3,5-lutidine) precursor.

To investigate whether or not the CdS xerogel can be synthesized with the sol−gel process under conventional drying, we spin-coated $L_2Cd(S(CO)CH_3)_2$ precursor solutions onto silicon wafers and characterized the CdS films, after baking, using X-ray diffraction (XRD), transmission electron microscopy (TEM), X-ray photoelectron spectroscopy (XPS), and ultraviolet−visible absorption spectroscopy. The precursor solutions were prepared by dissolving the cadmium precursor in pyridine. As mentioned above, the molecular precursor molecules are partially converted into the CdS nanoclusters, even at room temperature, and act as sol colloidal particles. It is the contention of the authors that in the actual precursor solution for the spin-coating process, there are diverse types of CdS species ranging from $L_2Cd(S(CO)CH_3)_2$ molecules to CdS nanoclusters with a diameter of ~5 nm. It is important to note that the thioacetic groups still exist on the surfaces of the CdS nanocluster and are easily condensable in the final, spin-coated films, a process typically viewed as aged in terms of the sol−gel reaction concept.[11]

To confirm the semiconducting properties of the thin CdS films, we fabricated metal−insulator−metal (MIM) structure devices and TFTs, as shown in Figure 2. The ZrO_2 gate dielectrics in the TFT device structure were prepared with a nonhydrolytic sol−gel method.[13]

Experimental Section

Materials. $L_2Cd(S(CO)CH_3)_2$ (*L* = 3,5-lutidine) was synthesized following the procedure described by Nyman et al.[12] All reagents were supplied by Aldrich Chemical Co. (St. Louis, MO, USA). Cadmium carbonate (99.999%), 3,5-lutidine (>98%), thioacetic acid (96%), and toluene (anhydrous, 99.8%) were used without further purification. Zirconium (IV) isopropoxide isopropanol complex (99.99%, $Zr(OCH(CH_3)_2)_4 \cdot (CH_3)_2CHOH$) and zirconium(IV) chloride (99.9+%) were used as received, as were the coating solvents of pyridine (anhydrous, 99.8%) and 2-methoxyethanol (anhydrous, 99.8%).

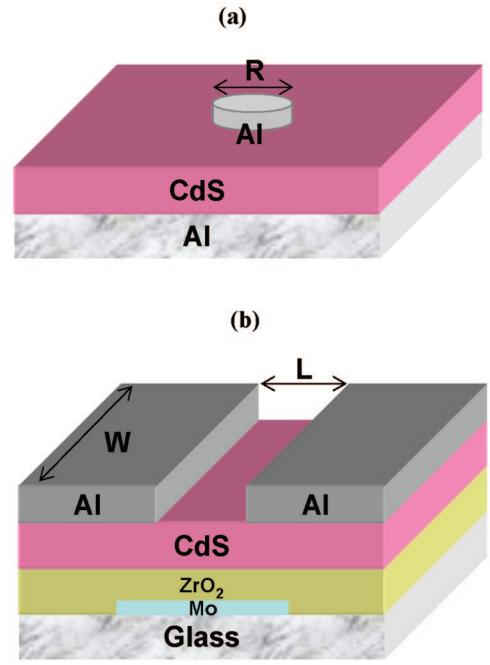

Figure 2. Schematic diagrams of the systems for measuring the electrical properties of the spin-coated thin CdS films. (a) The metal−insulator−metal (MIM) device structure used to measure the specific resistivity of the thin CdS films (CdS film thickness = 300−1700 Å). n^{+2}Si behaves similarly to metals; *D* (diameter) = 0.5 mm. (b) TFT device structure with a CdS channel and a ZrO_2 gate dielectric layer (CdS film thickness = 410 Å; ZrO_2 film thickness = 1490 Å; *L* (channel length) = 100 μm; *W* (channel width) = 1 mm).

Preparation of Thin CdS Films. The spin-coating process used to fabricate the thin CdS films consisted of 4 steps: (i) preparation of the $L_2Cd(S(CO)CH_3)_2$ precursor solution with a concentration of 9 wt.% (in pyridine); (ii) spin coating at 500 rpm in an air atmosphere onto silicon substrates; (iii) soft-baking with evaporation of the pyridine solvent by heating the thin films to 100 °C on a hot plate for 1 min, in a chamber where 10 sccm of nitrogen gas was mixed with ambient air; (iv) hard-baking of the thin films at 200 or 300 °C on a hot plate for 1 h in the same chamber and under the same conditions.

Device Fabrication. To investigate the electrical properties of the thin CdS films, metal−insulator−metal (MIM) devices were constructed, Figure 2a, in which through-film resistivity measurements were made between top and bottom Al electrodes. TFT devices were also fabricated as shown in Figure 2b. In both devices, the Al top electrodes were patterned with a metal shadow mask. In the TFT device structure, the Mo gate electrodes were patterned by photolithographic lift-off processes and the ZrO_2 gate dielectrics with a nonhydrolytic sol−gel method[13] consisting of 4 steps, similar to those used in the fabrication of the thin CdS films: (i) preparation of $ZrCl_4$ and $Zr(OCH(CH_3)_2)_4 \cdot (CH_3)_2CHOH$ precursor solutions with a concentration of 16 wt.% (in 2-methoxyethanol) and a molar ratio of 1:1; (ii) spin-coating at 500 rpm in an air atmosphere onto silicon substrates; (iii) soft-baking with evaporation of the 2-methoxyethanol solvent by heating the thin films to 100 °C on a hot plate in an air atmosphere for 1 min; (iv) hard-baking of the thin films at 300 °C on a hot plate in an air atmosphere for 1 h.

Characterization and Measurements. The thickness and refractive index of the thin CdS films were measured with a spectroscopic ellipsometer (M-2000V, J. A. Woollam Co. Inc.,

(13) Seon, J. B.; Jeong, H. D.;*et al.* to be submitted.

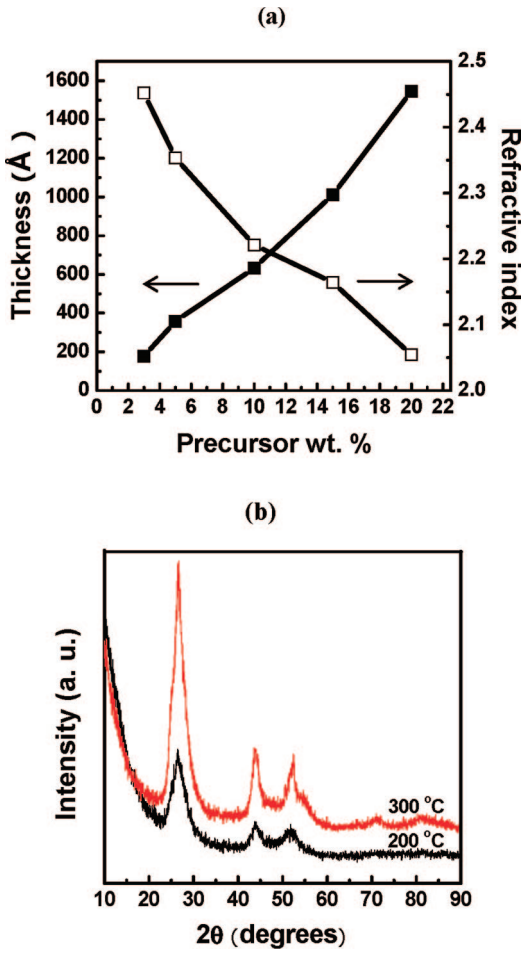

Figure 3. Thickness, refractive index, and XRD spectra of the spin-coated thin CdS films. (a) Variations in the thickness and refractive index of the CdS films hard-baked at 300 °C, with increases in the weight concentration (wt %) of the $L_2Cd(S(CO)CH_3)_2$ precursor solution. (b) XRD spectra of the CdS films hard-baked at 200 and 300 °C. The thickness of the CdS films is ~400 Å. The vertical lines on the *x* axis indicate the positions of the peaks of the hexagonal structure of CdS powder.

Lincoln, NE). The film crystallinity was measured with a Phillips X'pert Pro X-ray diffractometer equipped with a Cu Kα source at 40 kV and 30 mA. Two different hard-baking temperatures, 200 and 300 °C, were used to investigate the temperature dependence of the nanocrystallinity of the films. TEM analysis with a G2 FE-TEM Tecnai microscope was also used to determine the crystalline structures of the films. A XPS (PHI Q2000 system equipped with a monochromatized Al Kα (1486.6 eV) source provided the film composition. The dielectric constant of the ZrO_2 gate dielectric thin films was measured with the MIM structure using an Agilent 4284A precision LCR meter. Resistivity of the thin CdS films and characteristics of the TFTs were measured with a Keithley 4200 semiconductor characterization system in an air atmosphere.

Results and Discussion

With the spin-coating process, we succeeded in obtaining microscopically flat films with a thickness of several hundred angstroms and weight concentrations in the range of 3−20 wt % for samples hard-baked at 300 °C, as shown in Figure 3a. The roughness was measured with atomic force microscopy and found to be as small as 3.9 and 5.1 Å for films hard-baked at 200 and 300 °C, respectively. This exceptional uniformity is characteristic of xerogel films such as SiO_2. As mentioned in the discussion of the sol−gel reaction concept in the introduction, it would be useful to cross-reference the thermogravimetric analysis results of the $L_2Cd(S(CO)CH_3)_2$ (L = 3,5-lutidine) in the original paper,[12] wherein the thermal decomposition reaction is completed between 150 and 200 °C, indicating that the chemical reactions for the proposed film formation mechanism are completed for the 200- and 300 °C-baked thin films. In addition, it is evident that Figure 3a shows a strong thickness dependence of the refractive index of the CdS films. Though the exact model to account for the thicker films having the lower refractive index values is not at hand, its relation to a varying degree of solvent evaporation during the soft-baking process of the CdS xerogel films could be safely asserted. In the case of thicker films, escape from the film surface of the solvent molecules entrapped within the films is much more difficult, whereas the CdS networks are formed over the entire film area through the aging process. Solvent evaporation provides a capillary force within the pore surface, inducing the shrinkage of the network structure.[11] Thus, it is not unreasonable that as the amount of solvent molecules remaining after the soft-baking process increases, greater porosity is formed inside the films to give rise to lower refractive index values. Once the CdS skeletal networks involving the pore structure are formed, they are not significantly shrunk during the subsequent hard-baking step. Thus, the strong thickness dependence of the refractive index of the CdS films is important experimental evidence supporting the posited notion that the $L_2Cd(S(CO)CH_3)_2$ (L = 3,5-lutidine) precursor follows the xerogel-type film formation process due to the aforementioned sol−gel reaction.

CdS materials can exist in 2 crystalline forms, hexagonal and cubic structures.[14] XRD analysis indicates that the present spin-coated CdS films have a cubic crystalline structure, as shown in Figure 3(b). The broadness of the peaks in the XRD spectra is related to the size of the cubic crystalline phase. The full widths at half-maximum height of the peaks at $2\theta = 43.9°$, assigned to the (220) plane of the cubic crystalline structure, were observed to be 2.06 and 1.76 for the samples hard-baked at 200 and 300 °C, respectively. The Scherrer formula, $t = 0.9\,\lambda/\beta\cos\theta$, where λ is the wavelength of the incident X-rays, β the full width at half-maximum height, and θ the diffracted angle, was used to determine the crystalline domain size. These domain sizes were found to be 41 and 49 Å for the thin films hard-baked at 200 and 300 °C, respectively, indicating that the CdS nanocrystalline phases are embedded in the CdS films.

To confirm the presence of the nanocrystalline phase in the CdS films, TEM analysis was performed for a sample soft-baked at 100 °C and for samples hard-baked at 200 and 300 °C, as shown in Figure 4a−c, respectively. Figure 4d shows a TEM image of a thin CdS film spin-coated onto a Si substrate. In images b and c in Figure 4, the hard-baked films contain nanocrystalline domains with a size of approximately 5 nm, which is consistent with the XRD results. The formation of a CdS xerogel is confirmed by the pore

(14) Canava, B.; Gerard, I.; Guillemoles, J. F.; Lincot, D.; Etcheberry, A. *Thin Solid Films* **2005**, *480*, 230.

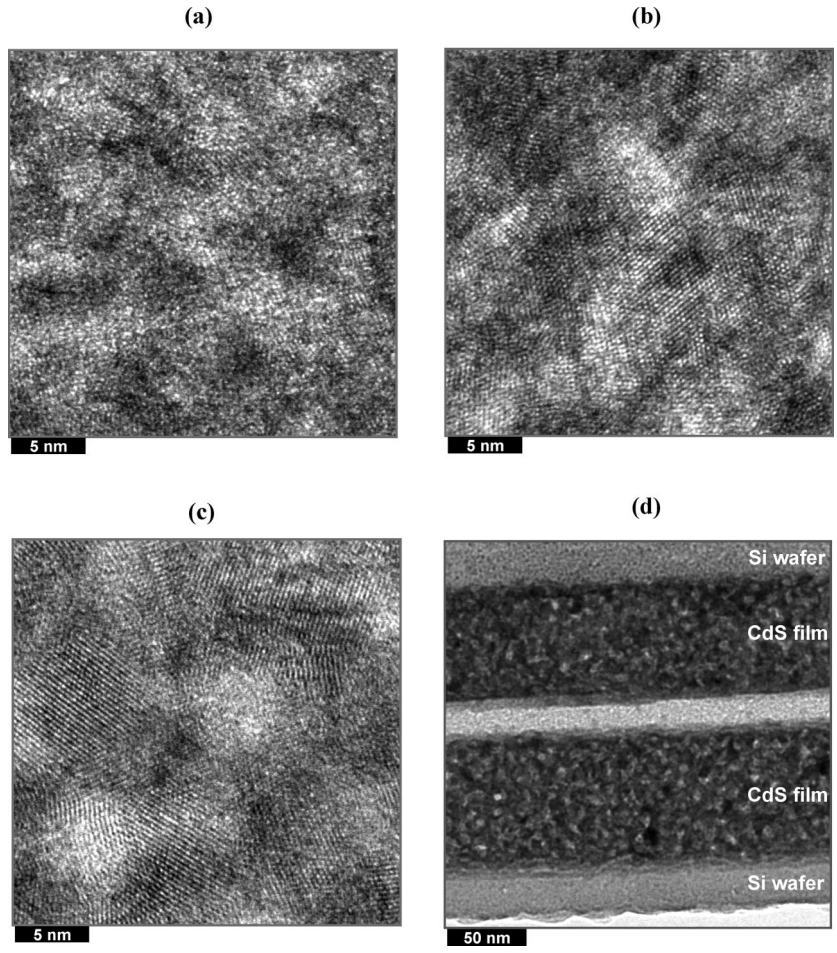

Figure 4. TEM images. (a) Sample soft-baked at 100 °C. (b, c) Samples hard-baked at 200 and 300 °C. (d) Thin CdS film spin-coated onto a Si substrate.

structures in the respective TEM images of the 2 samples cured at 200 and 300 °C, as shown in images b and c in Figure 4. The size of the pores in the white regions of the TEM images was estimated to be near 5 nm, without any significant difference between the pore sizes of the samples baked at 200 and 300 °C. The film density of the sample baked at 300 °C was found, with X-ray reflectivity measurements, to be 4.21 g/cm^3, and the porosity was calculated to be 13% with respect to a CdS bulk density of 4.83 g/cm^3. This porosity is significantly lower than that of SiO_2 xerogels and is probably due to the presence of nanocrystalline CdS phases, the density of which is surely the same as that of the bulk CdS.

The formation of Cd−S networks, leading to the formation of CdS films during the spin-coating process, can easily be understood given the above characterization results in terms of the concept of the conventional sol−gel reaction. During the soft-baking step at 100 °C, dissociation of the lutidine ligands and the elimination of thioacetic anhydride in the molecular precursors and CdS nanoclusters lead to the formation of a CdS nanocrystalline phase surrounded by the remaining $L_2Cd(S(CO)CH_3)_2$ molecules. The formation of the CdS nanocrystalline phase is supported by the TEM results for the film baked at 100 °C, as shown in Figure 4a. The authors suggest that the CdS nanocrystalline phase is capped with thioacetic groups that allow for subsequent intermolecular condensation, as shown in the schematic reaction in Figure 1. During the hard-baking step at 200 or 300 °C, the condensation polymerization of the capping groups of the CdS nanocrystals is completed. The CdS nanocrystalline phases are then converted from the wet gel state to the dry gel state in the soft- and hard-baking processes. In the wet gel state, the Cd−S−Cd networks are fully connected throughout the entire thin film, with the involvement of a small quantity of organic residues, such as pyridine, lutidine, and thioacetic anhydride molecules. The continued elimination of the organic residues results in the formation of the dry gel state (CdS xerogel), accompanied by the shrinkage of the CdS network.

Panels a and b in Figure 5 show the XPS depth profile results for the two films. Carbon and oxygen atoms were present in significant quantities on the surfaces of the CdS films, which were ascribed to the presence of hydrocarbon fragments containing oxygen atoms. In the bulk region of the two films, carbon and oxygen atoms are still observed. The respective concentrations of carbon and oxygen atoms are measured to be approximately 2.7 and 2.4% for the 200 °C baked sample, whereas the concentrations are 0.7 and 1.2% for the 300 °C baked sample. This unexpected presence of the atoms is likely due to a small amount of hydrocarbon fragments adsorbed only on the inner surface of the pore structure, not in the CdS nanocrystalline phases, given that the CdS nanocrystalline phases in the TEM results cannot exist if the carbon and oxygen atoms are intercalated in

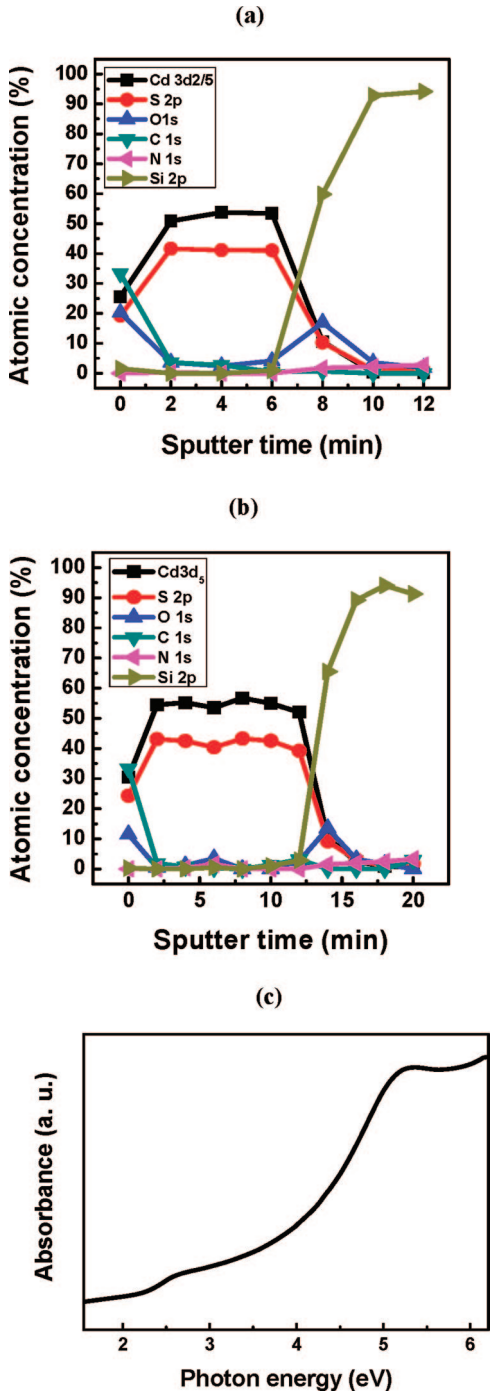

Figure 5. XPS and ultraviolet−visible spectroscopy results for the hard-baked thin CdS films. (a) XPS depth profile results: a sample hard-baked at 200 °C. (b) XPS depth profile results: a sample hard-baked at 300 °C. (c) Ultraviolet−visible spectroscopy results for the determination of the optical band gap: ultraviolet−visible absorption spectrum.

Cd−S−Cd−S− networks. Additionally, the hydrocarbon fragments on the pore structures would not significantly deteriorate the electrical properties of the porous CdS films that are solely dependent on the interconnected CdS network structures. As for the concentration of the oxygen atom, the concentration values of 2.4 and 1.2% are much smaller than those of the previously reported CdS films made by chemical bath reposition (CBD) and are in good agreement with the relatively excellent transistor characteristics soon to be discussed. Typically, in the CBD-CdS thin films, the concentrations of oxygen were reported to be in a range of 3−6 or 7−13%,[14,15] which were attributed to the CdO phase in the CdS films. This indicates that in the present nanocrystalline CdS films, there is less of a tendency to form the CdO phase. The concentration of carbon atoms in the CBD-CdS thin film was reported to remain very low, appearing just as traces in the XPS measurements,[14] whereas in the present CdS films, there is some carbon-related species due to the hydrocarbon fragments. The ratio of the atomic concentration of cadmium to that of sulfur in the bulk region of the film baked at 300 °C was measured to be 1.32; a value of 1.0 was obtained with Rutherford backscattering spectroscopy measurements. The lower intensity of the sulfur atoms in the XPS measurements is probably due to the preferential etching of these atoms during Ar^+ ion sputtering in the depth profiling process. Nevertheless, a Cd:S ratio of 1.32 is still much lower than the previous 1.56 of the CBD-CdS thin film.[15] This is related to the lower concentration of oxygen atoms in the CdS thin film and is why, as initially planned, the condensation mechanism of the $L_2Cd(S(CO)CH_3)_2$ (L = 3,5-lutidine) precursor retains the original Cd−S bond, while in the CBD methods, new Cd−S bonds have to be made from precursors such as $Cd(NH_3)_4^{2+}$, with partially made Cd−O bonds.

We performed ultraviolet−visible absorption spectroscopy on the sample hard-baked at 300 °C. The first absorption peak in Figure 5c is used to quantify the effective band gap that occurs at ~2.7 eV. According to the previous investigation of the relation between nanocrystal size and band gap in CdS crystallites,[16] CdS nanocrystals with a size of 4−6 nm should have a band gap value in the range 3.0−2.7 eV. This correlates well with the XRD and TEM results indicating that the size of the nanocrystalline domain is roughly 5 nm for the hard-baked 300 °C film.

One of the most important issues of the porous nanocrystalline CdS films is whether they are semiconducting or insulating in terms of electrical properties. This is because the nanocrystalline phases are embedded in the amorphous phases, which may act an energy barrier, interrupting the formation of electron band structures of long-range order. It is possible that the nanocrystalline CdS phases are electrically isolating, giving rise to the poor electrical characteristics; however, it is the view of the authors that the electrical characteristics of the CdS films are similar to those of conventional CdS films because of the following reasons. It has been reported that the exchange interactions between metallic and semiconducting nanocrystals endow conducting or semiconducting properties, where the exchange coupling energy scales approximately as $\beta \approx \exp[-\kappa(d + \delta)]$, where d is the nanocrystal diameter, δ the interparticle spacing, and κ^{-1} describes the length scale of the wave function leakage outside the nanocrystal.[9,16] Therefore, if the interparticle spacing (δ) is <20% of the diameter (d), then the wave functions of the valence electrons overlap significantly and the nanocrystals are exchange coupled.[17] As shown in images

(15) Maliki, H. E.; Bernede, J. C.; Marsillac, S.; Pinel, J.; Castel, X.; Pouzet, J. *Appl. Surf. Sci.* **2003**, *205*, 65.
(16) Brus, L. E. *J. Chem. Phys.* **1984**, *80*, 4403.
(17) Remacle, F.; Beverly, K. C.; Heath, J. R.; Levine, R. D. *J. Phys. Chem. B* **2003**, *107*, 13892.

b and c in Figure 4, in the present CdS films, because the amorphous CdS phases are very thin (whose thickness ranges over from sub nanometer to a few nanometers), there must be many chances to manifest the exchange interactions, allowing for excellent semiconducting properties.

The electrical properties of the CdS xerogel films were then investigated, with focus upon electrical resistivity and field effect mobility of the films, which are the most important prerequisites for their use in TFTs. The current−voltage characteristics were measured using the Al-CdS-Al MIM structure, Figure 2a, for the films with varying thickness obtained by hard-baking at 300 °C, as shown in Figure 6a. The specific resistivity for a thickness of 1000 Å was estimated to be about 800 Ω cm, which is within the range 1×10^{-2} to 1×10^{9} Ω cm for conventional semiconductors. The resistivity is inversely proportional to the film thickness. This trend can be explained by noting that the resistivity of the interface region is greater than that of the other bulk regions,[18] which is attributed to the surface scattering of charge carriers in the interface region. The electrical resistivity of a semiconductor is generally dependent on the carrier concentration and the mean free path of the charge carriers. When a semiconductor sample is sufficiently thin, its thickness is comparable to the mean free path of the charge carriers and the surface scattering is enhanced.[19] To extract the bulk film resistivity distinct, the thickness dependent resistivity data are further analyzed. The bulk resistivity is extracted by the fitting the data and taking the limit of infinite film thickness. In the current analysis, the bulk resistivity is estimated to 454 Ω cm, which is not quite different of that (744 Ω cm) of a previous study,[20] involving the CdS films were prepared by the chemical vapor deposition (CBD).

To measure the field-effect mobilities of the spin-coated CdS films, we employed TFTs, with an inverted structure consisting of Mo as the bottom gate electrode and solution-processed ZrO_2 as the gate dielectric layer, as shown in Figure 2b. Representative plots of the drain current, I_{DS}, versus the drain voltage, V_{DS}, are shown in Figure 6b for various applied gate voltages, V_{GS}, for a sample hard-baked at 300 °C, with a thickness of about 410 Å. These output characteristics are typical of field effect transistors for positive V_{DS}. The current saturates at a certain value of V_{DS} that depends on the gate voltage. In Figure 6c, for a V_{DS} of 5 V in the saturation region, the drain current, I_{DS}, is plotted as a function of V_{GS}. From the linear fits in Figure 6c, the field-effect mobility, μ, in the saturation regime was determined with the following equation, as given by the conventional metal-oxide-metal semiconductor field-effect transistor model[21]

$$I_{DS} = \frac{WC_i\mu}{2L}(V_{GS} - V_T)^2 \quad (3)$$

where C_i is the areal capacitance of the ZrO_2 insulator, W is the channel width, L is the channel length, V_T is the threshold voltage, and μ the field-effect mobility. The ZrO_2 gate insulator has a high dielectric constant of about 10 at 100 kHz.[13]

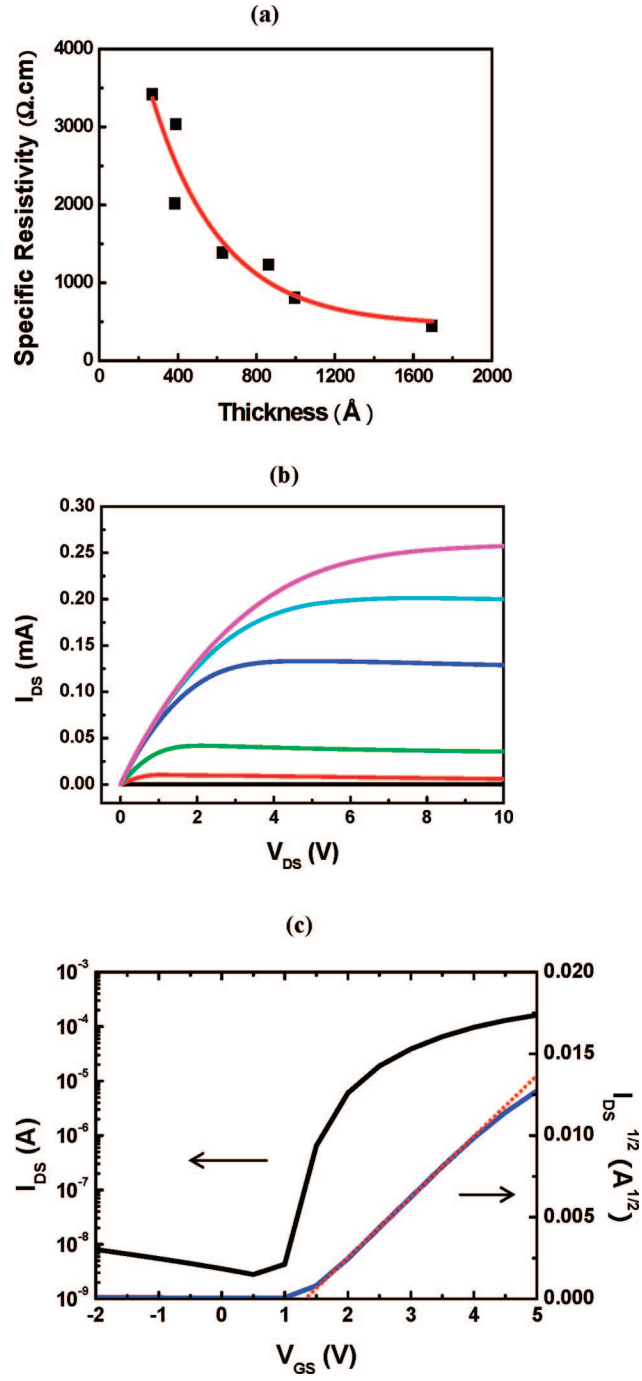

Figure 6. Electrical properties of the thin CdS films. (a) Thickness dependence of the specific resistivity. As the thickness is reduced, the specific resistivity of the film increases abruptly in the experimental thickness range. (b) Output characteristics: I_{DS} versus V_{DS} for various V_{GS}. (c) Transfer characteristics: I_{DS} versus V_{GS} for constant V_{DS} (V_{DS} = 5 V). The gate dielectrics are solution-processed 1490 Å ZrO_2. The CdS thickness is ~410 Å. The channel width and length are 1 mm and 100 μm, respectively. A saturation mobility of 48 $cm^2\ V^{-1}\ s^{-1}$, an on/off ratio of 1.7×10^5, and a threshold voltage of 1.3 V were obtained.

(18) The resistivity of an interface region ($\rho_{surface}$) with a thickness of λ is different from that of a bulk region (ρ_{bulk}) with a thickness of $d-2\lambda$, where the film thickness is d. With these notations, the additive rule of serial resistance can be applied. Here, A is the area of the top electrode of the sandwich structure. $\rho_{film}(d/A) = 2\rho_{surface}(\lambda/A) + \rho_{bulk}(d-2\lambda)/A$. Therefore, $\rho_{film} = \rho_{bulk} + 2(\rho_{surface}-\rho_{bulk})(\lambda/d)$. Thus, it is possible to show with this simple argument that the resistivity varies linearly with the reciprocal thickness.

(19) Wilson, J. I. B.; Woods, J. *J. Phys. Chem. Solids* **1973**, *34*, 171.
(20) Chang, Y. J.; Munsee, C. L.; Herman, G. S.; Wager, J. F.; Mugdur, P.; Lee, D. H.; Chang, C. H. *Surf. Interface Anal.* **2005**, *37*, 398.
(21) Kagan, C. R.; Andry, P. *Thin-Film Transistors*; Marcel Dekker, New York, 2003.

The field-effect mobility under saturation conditions (μ_{sat}) is then calculated from the slope of the plot of $I_{DS}^{1/2}$ versus V_{GS}. From the data in Figure 6c, a field-effect mobility in the saturation region (μ_{sat}) of 48 $cm^2\ V^{-1}\ s^{-1}$, a threshold voltage of 1.3 V, and an on/off current ratio of 1.7×10^5 were obtained. Further, the subthreshold slope was calculated to be 0.2 V/decade. As can be best ascertained, this field-effect mobility is superior to those of all previously reported solution-processed TFT devices, including those with an organic or an inorganic channel layer produced with low temperature processing. In the Duan study, it was reported that the mobilities of the solution-processed Si nanowire and CdS nanoribbon devices exceed 100 cm^2/Vs,[22] where Si nanowire and CdS nanoribbon films were deposited using a fluidic flow alignment approach.[23] However, as discussed in the Mitzi study,[7] these results were obtained from discrete nanowires across the electrodes, rather than for a continuous film, and the mobility value >100 cm^2/Vs was based on an effective channel width calculated using the nanowire diameter multiplied by the number of wires crossing the channel. Therefore, in the true channel width of the device, the nanowire devices yield a mobility approximately 2 orders of magnitude smaller than the mobility value of 12.0 $cm^2\ V^{-1}\ s^{-1}$ reported in the Mitzi study.[7] This is the reason why the mobility value (48 $cm^2\ V^{-1}\ s^{-1}$) obtained with the current CdS films is thought to be the highest in the solution-processed inorganic semiconductor thin films. It would come as little surprise that the mobility value seems to be too high, when considering that the CdS nanocrystalline domains were surrounded with the amorphous phases that might interrupt electron transport between the nanocrystalline domains. However, as already discussed, the assertion put forth that there are significant exchange interactions between the semiconducting nanocrystalline domains, where the wave function leakage outside the nanocrystal allows electronic communication between them. In addition, it is the contention of the authors that the highest mobility value is likely to be in part due to the ZrO_2 gate insulator synthesized by using the nonhydrolytic method, though this has not been seriously studied yet. Instead of the ZrO_2 thin films, conventional PECVD SiO_2 thin films had been first used as the gate insulator of the current CdS TFT devices, where the threshold voltage ranged from 50−100 V and the mobility value was limited to less than 5 $cm^2\ V^{-1}\ s^{-1}$. This is thought because, compared to the PECVD SiO_2 thin films, the ZrO_2 thin films induce the more effective charge accumulation at the channel region of the CdS semiconducting film adjacent to the ZrO_2/CdS interface. The planning of extensive studies of the ZrO_2/CdS interface with surface science point of view, in order to investigate the high compatibility of the nonhydrolytic ZrO_2 thin film with the semiconductor thin film of the CdS xerogel material is underway.

(22) Duan, X.; Niu, C.; Sahl, V.; Chen, J.; Parce, J. W.; Empedocles, S.; Goldman, J. L. *Nature* **2005**, *425*, 274.
(23) Huang, Y.; Duan, X.; Wei, Q.; Lieber, C. M. *Science* **2001**, *291*, 630.

Summary

In this study, the fabrication of new solution-processed inorganic materials that enable the production of devices with both low-cost processability and excellent characteristics, better than those of other organic and inorganic channel materials, have been demonstrated. With a sol−gel process, microscopically flat, thin CdS xerogel films were successfully obtained. These films were found to consist of a nanocrystalline phase with 5 nm crystal domains and to have good film uniformity. The specific resistivity of the films was found to be within the range of values of conventional semiconductors. A device fabricated with a CdS channel and a ZrO_2 gate dielectric layer was found to have a field effect mobility of 48 $cm^2\ V^{-1}\ s^{-1}$, a threshold voltage of 1.3 V, an on/off current ratio of 1.7×10^5, and a subthreshold slope of 0.2 V/decade. This field-effect mobility is better than that of any other solution-processed organic or inorganic semiconductor TFT reported thus far. In addition, its low operation voltage (<5 V) means that it has low power consumption. The current study provides a general and rational approach to the fabrication of low-cost and high-performance solution-processed inorganic TFTs and opens up new possibilities in the field of printable and flexible electronics.

Acknowledgment. This work was originally planned and financially supported by the Samsung Advanced Institute of Technology. The authors greatly acknowledge its research staff for helpful discussions.

CM801557Q